

Naval Surface Warfare Center

Carderock Division

West Bethesda, MD 20817-5700

NSWCCD-61-TR-1999/02 February 1999

Survivability, Structures, and Materials Directorate
Technical Report

Effects of Inclusions and Austenite Grain Size on the Impact Behavior of a Newly Developed Low-Carbon Steel Weld Metal

by

J. M. Blackburn, A. Brandemart, and A.G. Fox

CARDIVNSWC-61-TR-99/02 EFFECTS OF INCLUSIONS AND AUSTENITE GRAIN SIZE ON THE IMPACT BEHAVIOR OF A NEWLY DEVELOPED LOW-CARBON STEEL WELD METAL



DTIC QUALITY INSPECTED 2

Approved for public release; distribution is unlimited

19991215 021

Naval Surface Warfare Center

Carderock Division

West Bethesda, MD 20817-5700

NSWCCD-61-TR-1999/02 February 1999

Survivability, Structures, and Materials Directorate
Technical Report

**Effects of Inclusions and Austenite Grain Size on the Impact Behavior of a Newly
Developed Low-Carbon Steel Weld Metal**

by

J. M. Blackburn, A. Brandemart, and A.G. Fox

Approved for public release; distribution is unlimited

REPORT DOCUMENTATION PAGE			Form Approved OMB No. 0704-0188
1. AGENCY USE ONLY (Leave blank)	2. REPORT DATE 2/11/99	3. REPORT TYPE AND DATES COVERED Research and Development 971001-980931	
4. TITLE AND SUBTITLE EFFECTS OF INCLUSIONS AND AUSTENITE GRAIN SIZE ON THE IMPACT BEHAVIOR OF A NEWLY DEVELOPED LOW-CARBON STEEL WELD METAL			5. FUNDING NUMBERS 1-6150-953
6. AUTHOR(S) J.M. Blackburn, A. Brandemart, A.G. Fox			8. PERFORMING ORGANIZATION REPORT NUMBER TR-61-TR-1999/02
7. PERFORMING ORGANIZATION NAME(S) AND ADDRESS(ES) Naval Surface Warfare Center, Carderock Division Code 615 9500 MacArthur Blvd West Bethesda, MD 20817-5700			
9. SPONSORING/MONITORING AGENCY NAME(S) AND ADDRESS(ES) ONR 332 Office of Naval Research Arlington, VA 22217-5000			10. SPONSORING/MONITORING AGENCY REPORT NUMBER
11. SUPPLEMENTARY NOTES			
12a. DISTRIBUTION/AVAILABILITY STATEMENT Approved for public release; distribution is unlimited.			12b. DISTRIBUTION CODE Statement A
13. ABSTRACT (Maximum 200 words) Inclusion characteristics were altered using intentional oxygen gas additions in GMA welds. Specimens removed from the deposited weld metal were subjected to grain refinement by thermal cycling to 1100°C for up to 3 cycles using the Gleeble 1500. Each successive cycle resulted in additional grain refinement. By systematically varying the oxygen and grain size, the effects of inclusions and grain size on the impact toughness behavior of low carbon steel weld metal was determined. It was concluded that austenite grain refinement was effective at improving toughness across the entire test temperature region, with the exception of the upper shelf energy when the inclusion count and volume fraction were the largest. Although grain refinement resulted in improved toughness, it was concluded that inclusions were the primary factor limiting toughness improvement. It was also concluded that the as-deposited columnar grain structure remaining in the weld metal was somewhat responsible for the lower toughness regions within the weld.			
14. SUBJECT TERMS			15. NUMBER OF PAGES
			16. PRICE CODE
17. SECURITY CLASSIFICATION OF REPORT Unclassified	18. SECURITY CLASSIFICATION OF THIS PAGE Unclassified	19. SECURITY CLASSIFICATION OF ABSTRACT Unclassified	20. LIMITATION OF ABSTRACT Unclassified

TABLE OF CONTENTS

ABBREVIATIONS	vi
ABSTRACT	1
ACKNOWLEDGEMENTS	1
INTRODUCTION.....	1
OBJECTIVE	2
APPROACH	2
RESULTS AND DISCUSSION	2
CHEMICAL ANALYSIS, 50% TRANSFORMATION TEMPERATURE, AND STRENGTH.....	2
INCLUSIONS.....	3
AUSTENITE GRAIN WIDTH (γ_w).....	3
MICROSTRUCTURAL ANALYSIS	3
HARDNESS	3
CVN IMPACT TESTING.....	4
REGRESSION MODEL	4
CONCLUSIONS	5
REFERENCES.....	6
APPENDIX A –CVN DATA SHOWING THE EFFECTS OF REHEATING.....	19
APPENDIX B –CVN DATA SHOWING THE EFFECTS OF OXYGEN (CONT'D).....	22

LIST OF TABLES

TABLE I. TEST DESIGN MATRIX.....	7
TABLE II. CHEMICAL COMPOSITION, TENSILE PROPERTIES, AND 50% TRANSFORMATION TEMPERATURES.....	8
TABLE III. REGRESSION STATISTICS FOR 50% FATT.....	8

LIST OF FIGURES

FIGURE 1. THE EFFECT OF WIRE OXYGEN ON WELD METAL DEPOSIT OXYGEN.....	9
FIGURE 2. SUMMARY OF INCLUSION DATA.....	10

FIGURE 3. THE EFFECT OF WELD METAL OXYGEN ON INCLUSION CHARACTERISTICS. .	11
FIGURE 4. AUSTENITE GRAIN WIDTH (γ_w) SUMMARY.....	12
FIGURE 5. MICROGRAPHS OF WELD METAL CONDITIONS.....	13
FIGURE 6. WELD METAL HARDNESS PROFILES WITH SHIELDING GASES CONTAINING AR AND 2,5 OR 10% O ₂	14
FIGURE 7. FACTORS AFFECTING 50% FATT.	15
FIGURE 8. FACTORS AFFECTING USE.....	16
FIGURE 9. FACTORS AFFECTING LSE.....	17
FIGURE 10. 50% FATT MODEL.	18

Abbreviations

CVN	Charpy vee notch	HSLA	High strength low alloy
°C	Degrees Centigrade	LSE	Lower shelf energy
d_{avg}	Average inclusion diameter	mm	millimeters
DPH	Diamond pyramid hardness	μm	micrometers
J	Joules	Mpa	MegaPascal
FATT	Fracture appearance transition temp.	ppm	Parts per million
γ_w	Austenite grain width	T ₅₀	50% transformation temperature
GMA	Gas metal arc	USE	Upper shelf energy
GMAW	Gas metal arc welding	UTS	Ultimate tensile strength
		V _f	Volume fraction of inclusions
		YS	Yield strength

Abstract

Inclusion characteristics were altered using intentional oxygen gas additions in GMA welds. Specimens removed from the deposited weld metal were subjected to grain refinement by thermal cycling to 1100°C for up to 3 cycles using the Gleeble 1500. Each successive cycle resulted in additional grain refinement. By systematically varying the oxygen and grain size, the effects of inclusions and grain size on the impact toughness behavior of low carbon steel weld metal were determined. It was concluded that austenite grain refinement was effective at improving toughness across the entire test temperature region, with the exception of the upper shelf energy, when the inclusion count and volume fraction were the largest. Although grain refinement resulted in improved toughness, it was concluded that inclusions were the primary factor limiting toughness improvement. It was also concluded that the as-deposited columnar grain structure remaining in the weld metal was somewhat responsible for the lower toughness regions within the weld.

Acknowledgements

This work was sponsored by ONR, Dr. George Yoder (ONR Code 332). This work was part of the ONR Seaborne Structural Materials Project.

Introduction

Substitution of HSLA-steels for HY-steels in surface ship construction has provided substantial cost savings to the Navy, primarily through reduction of preheat. HSLA-steels are currently welded with filler metals developed more than 25 years ago for use with HY-steels. In response to the need to match the superior weldability of HSLA steels, the U.S. Navy is conducting a program to develop and certify improved filler metals for welding of HSLA and HY steels [1]. The primary emphasis is currently on developing new solid wires for GMA welding of HSLA and HY-steels. The intended strength range is from 565 to 793 MPa while obtaining CVN impact values as high as 61 joules at -51°C. The mechanical property targets are identical to those specified for currently-available products (Mil-100S-1 and Mil-120S-1). The technological change is in the operational requirements, developing wires that are cooling-rate insensitive and can be welded without preheat/interpass controls.

It is well known that inclusions can affect cleavage and ductile fracture. It has been shown that particles, such as carbides and inclusions can initiate cleavage. [2,3] Larger particles are usually associated with cleavage initiation since the stress intensity, in a given stress field, is higher for a longer crack in a cracked particle. It has been demonstrated that inclusions in the uppermost end of the size distribution ($>1\mu\text{m}$) are responsible for cleavage initiation in weld metal. [4] However, it is not likely that the growth of a cleavage crack is influenced by inclusions. Ductile fracture, on the other hand, occurs by the growth and coalescence of micro-voids nucleated at inclusions. [5] Ductile crack growth is promoted by increased size and decreased separation of inclusions. Therefore, an increasing volume fraction of inclusions represents a higher likelihood of ductile crack initiation and propagation.

A finer ferrite grain size increases the resistance to cleavage due to the fact that in a finer grained material the cleavage crack must change direction more often to continue cleavage along $\{100\}$ planes [6], thus providing for a more tortuous fracture path. Since the ferrite grain size is related to the prior austenite grain size in weld metal [7], this relationship can also hold true as a function of austenite grain size.

Oxygen data collected throughout the entire weld metal development program are plotted in Figure

1 for welds made with 95%Ar - 5%CO₂ shielding gas. Although a different shielding gas was used in the work to be reported below, the trend of increasing deposit oxygen can be expected. It can be seen that increasing wire oxygen content increases the oxygen in the weld deposit. Weld deposit oxygen levels up to 0.030% can be expected when welding with air melted wire in the GMAW process. As will be seen later in this paper, the resulting oxygen content of the deposited weld metal relates to the inclusion size and volume fraction. It will be shown that these inclusion characteristics greatly influence the toughness performance.

Objective

The objective of this work was to quantify the effects of inclusions and austenite grain size on the CVN impact toughness. The importance of quantification relates to the ongoing development of these new wires. The experimental heats of wire were vacuum induction melted and contain very low levels of oxygen and nitrogen. The production heats will be air-melted, and will thus contain higher levels of oxygen and nitrogen. The effects of nitrogen on similar materials have been reported previously. [8] The quantification of oxygen effects in this study will provide valuable information relative to the performance of future production heats with increased oxygen levels.

Approach

The purpose of this investigation was to quantify the effects of inclusions and austenite grain size on the CVN impact toughness. In order to vary the inclusion distribution characteristics, intentional oxygen gas additions were made to GMA welds. The welds were fabricated in an HSLA-100 steel using a heat input of 2362 J/mm and argon/oxygen shielding gas mixtures of 2%, 5%, and 10% oxygen. Each material, with varying amounts of oxygen and inclusions, was subjected to grain refinement by thermal cycling to 1100°C for up to 3 cycles using the Gleeble 1500. The thermal cycle for a peak temperature of 1100°C was calculated using the Rykalin model [9] for a weld heat input of 2362 J/mm. By systematically varying the oxygen to 3 different levels and grain size to 4 different levels, a matrix was developed which allowed for the determination of the independent and combined effects of inclusions and grain size on the fracture behavior of low carbon steel weld metal. The matrix of material conditions is reported in Table I.

In order to quantify the effects of grain size, microstructure and inclusions, the following was performed on the as deposited weld metals and the cycled weld metal specimens: (a) chemical analysis, (b) precision dilatometry (to determine the 50% transformation temperatures), (c) tensile testing (d) microstructural analysis (e) inclusion distribution characteristics (using the SEM), (f) austenite grain width measurements, (g) micro-hardness measurements, and (h) CVN impact testing.

Results and Discussion

Chemical Analysis, 50% Transformation Temperature, and Strength

The composition, tensile properties, and 50% transformation temperature of the materials used in this investigation are reported in Table II. Additions of 2%, 5%, and 10% oxygen to the shielding gas resulted in weld metal oxygen levels of 220, 260, and 470 ppm. As a result of the increased oxygen levels some de-alloying also occurred, most notably C and Mn. Because of the decreased hardenability, the strength was also reduced. The decreased hardenability was also reflected in an increase in the 50% transformation temperature. This is consistent with the strength results, in that lower temperature transformation products generally produce higher strengths. These transformation temperatures did not vary as a function of the number of thermal cycles.

Inclusions

The results of the inclusion analysis are reported in Figure 2. The distribution for 2% oxygen contains the highest number of inclusions at the smallest inclusion sizes. As oxygen increased to 5% and 10%, the number of inclusions decreased and shifted to larger diameters. The number of inclusions exceeding 1 micron increased significantly when the shielding gas oxygen was greater than 2%.

Figure 3 relates the weld metal oxygen to the inclusion characteristics. Inclusion volume fraction (V_f) and average diameter (d_{avg}) increased linearly as a function of the weld oxygen content. Since wire oxygen content is related to deposit oxygen content (Fig. 1), increases in wire oxygen content due to air melting is expected to increase both inclusion size and volume fraction.

Austenite Grain Width (γ_w)

The results of austenite grain width measurements are shown in Figure 4. The bars represent the range of values obtained. The as-welded condition produced austenite grain widths in the range of approximately 250 to 475 microns. The range of grain widths increased as a function of increasing oxygen content. The mean grain widths, for the as-welded condition, suggest a slight increase in width moving from 5% to 10% oxygen. Subsequent thermal cycling to 1100°C resulted in significant austenite grain refinement. A single cycle produced the highest degree of refinement in all cases to values of approximately 25 microns with very little variation. The second and third cycles produced further refinement by only a few microns to around 20 microns, and resulted in reduced variation.

Microstructural Analysis

Representative optical micrographs for each condition within the test matrix are shown in Figure 5. The as-welded microstructures welded with 2% oxygen was the finest of the microstructures displaying a mixture of martensite, lath ferrite, acicular ferrite and polygonal ferrite. The dark etching regions are martensite aligned on solidification boundaries. This martensite probably resulted from solute dumping during solidification which produced these more highly alloyed regions. As oxygen was increased the as-welded microstructures contained increasing amounts of coarser regions and contained primarily lath ferrite with decreasing amounts of martensite. The increased oxygen in the shielding gas resulted in some de-alloying in the system resulting in fewer areas of martensite production.

As each of the as-welded structures were thermally cycled to 1100°C, refinement in the microstructure was evident. However, the most refinement occurred after only a single thermal cycle, as indicated previously by the prior austenite grain width data. Additional cycling did not result in significant additional refinement. The microstructures of the thermally cycled weld metals experienced a reduction in the number of localized areas of martensite and an increase in acicularity. The amount of acicularity appears to decrease with increasing amounts of oxygen.

Hardness

The hardness profiles of a weld bead and its associated reheated regions for each of the 3 welds are given in Fig. 6. As the amount of oxygen in the shielding gas increased, the hardness decreased. This is due to the de-alloying, and decreased hardenability. The different regions within the weldment are delineated. The hardest zones are that of the non-reheated weld metal and the area within the recrystallized zones. The areas outside of the recrystallized zone, or the tempered region, showed a significant amount of softening.

The averages of 20 hardness indentations of each thermally cycled sample are given in Table I along with the range of hardness experienced within the weldment itself. This data shows no substantial difference in hardness with increasing number of thermal cycles. However, the hardness generally decreased as a function of the amount of oxygen in the shielding gas, as in Fig. 6. Upon comparing the hardness of the thermal cycled specimens to the range of the hardness in the weldment, it can be seen that the hardness of the cycled specimens fall near the upper end of the weldment hardness range. This is

reasonable since the thermal cycles simulated the high temperature regime of a reheated region. It can be concluded from this data that the cycled specimens are a reasonable simulation of the high temperature reheated region of the deposited weld metal.

CVN Impact Testing

The systematic variation of oxygen and grain refinement permitted the investigation of the independent effects of inclusions and grain size on the impact toughness. Table I presents the matrix of conditions. Figures 7, 8 and 9 summarize the results of CVN impact testing. Complete results for CVN impact testing are given in Appendices A and B. Figure 7 shows the effect of austenite grain width and inclusions (d_{avg} and V_f) on the 50% FATT. Reduction of the grain width resulted in considerable improvement in the FATT in all cases. The most significant improvement was in the cases where the V_f was 0.18 or 0.22. The improvement was approximately -30°C . In the case where the V_f was 0.41, the improvement in the FATT was not as significant. The improvement in this case was about -15°C . Figure 7 also shows that increasing the number and size of inclusions while holding the austenite grain width fixed resulted in an increase in the FATT. It is clear from Figure 7 that the improvement effects due to grain refinement is limited by the presence of inclusions.

Figure 8 shows the effect of austenite grain width and inclusions on the upper shelf energy (USE). Some increase in upper shelf was obtained as a result of refining the grain size for the data with inclusion V_f of 0.18 and 0.22. For inclusion V_f of 0.41, no change in USE was observed. It can also be seen that fewer and smaller inclusions result in a higher USE at a given grain width. It is evident from Figure 8 that austenite grain width has minimal effect on USE. As the inclusion content increased, the effect of grain refinement on upper shelf diminished to zero. The slight improvement in upper shelf, due to decreasing grain width, is probably due to slight increases in strength as a result of grain refinement. However, this effect is diminished as the inclusions increase in size and population.

Figure 9 presents the effect of austenite grain width and inclusions on the lower shelf energy (LSE). The LSE was determined at 10% ductile fracture appearance. The data points with the arrows indicate that the LSE was lower than that represented by the data point. In those cases, this was the lowest energy obtained at a test temperature of -66°C and fracture appearances of approximately 30% to 40% ductility.

Refinement of the grain size resulted in an enhancement of the LSE. The enhancement was the greatest for the specimens with an inclusion V_f of 0.18. This effect was decreased with increasing V_f , but not totally. Unlike upper shelf behavior, the improvement in toughness was not due to an increase in strength. Increased strength would decrease the lower shelf. [10] Therefore, it is purely a result of the grain refinement. Figure 9 also shows that the inclusions limit the toughness on the lower shelf. The specimens with the fewest and smallest inclusions resulted in a higher LSE. Inclusions and grain width also had a pronounced effect on the lower shelf toughness.

In summary, it was shown that increasing inclusion content resulted in a degradation of the CVN impact toughness and decreasing austenite grain width was effective in increasing the overall impact toughness performance of low carbon steel weld metal. Austenite grain refinement was effective at improving the toughness across the entire test temperature region with the exception of the USE when the inclusion count and volume fraction were the largest. Although grain refinement resulted in improved toughness, it was shown that inclusions were the primary factor limiting toughness enhancement. Since grain refinement improves toughness, it can be inferred that the as-deposited columnar grain structure was somewhat responsible for the lower toughness regions within the weld.

Regression Model

The 50% FATT was successfully predicted from the prior austenite grain width (γ_w), and the volume

fraction of inclusions(V_f). The resulting regression terms are shown in Eqn. 1 and the model visualized in Figure 10. As is frequently the case, the best fit model involved the inverse square root of the grain width. In this case it is prior austenite grain width, where in many studies on fracture it is ferrite grain size [11]. However, in this case austenite grain width and ferrite grain size are probably related in a positive manner. As described in the "microstructure" section it was observed that as the austenite grain width was refined, the resulting final structure also became finer. It was not determined whether or not the prior austenite grain width directly contributed to fracture therefore γ may be an indirect measure of the specific features related to the fracture process.

$$50\% \text{ FATT}(\text{°C}) = -151 + 135(V_f) - 21[\ln(\gamma_w)^{-0.5}] \quad \text{Eqn. 1}$$

The statistics associated with the regression of Eqn. 1 are shown in Table III. The values represented in this table indicate that the terms are highly significant and the prediction is of reasonably good accuracy.

Conclusions

The objective of this work was to quantify the effects of inclusions and austenite grain size on the CVN impact toughness. It was concluded that increasing inclusion content resulted in a degradation of the CVN impact toughness and that decreasing austenite grain width was effective in increasing the overall impact toughness performance of low carbon steel weld metal. Austenite grain refinement was effective at improving the toughness across the entire test temperature region with the exception of the upper shelf energy when the inclusion count and volume fraction were the largest. Although grain refinement resulted in improved toughness, it was concluded that inclusions were the primary factor limiting toughness enhancement. This also led to the conclusion that the as-deposited columnar grain structure is one factor accounting for the lower toughness regions within an as-deposited weld.

References

1. DeLoach, J.J. 1996., Welding and Weld Automation in Shipbuilding: Proc. Materials Week '95 conf. ed. R.DeNale. TMS, pp. 85-104.
2. McMahon, C.J. and M. Cohen, *Acta Metall.*, 1965, 13, 1401.
3. Tweed, J.H. and J.F. Knott, *Acta Metall.*, 1987, 35, 1401.
4. Hughes, R.K., and J.C. Ritter, *Trends in Welding Res.*, Proc. of the 4th Int. Conf., 5-8 June 1995, ASM International, pp 645-650.
5. Chin, J, *Weld. J.*, 1969, 48, 290s-294s.
6. Honeycombe, R.W.K., *Steels, Microstructure and Properties*, ASM, 1981, p.186.
7. Umemoto, Aing Hai Guo, & Tamura, *Mat. Sci. and Tech.*, 1987, 3(4), , pp 249-255.
8. Blackburn, J., and J. DeLoach, "The Effects of Nitrogen on ULCB Steel Weld Metal," *Proceedings of the International Conference on Advances in Welding Technology*, EWI, Columbus, OH, Nov. 6-8, 1996.
9. Ferguson, H.S., D.L. Hollinger, *Trends in Welding Res.*, Proc. of the Int. Conf., 18-22 May 1986, ASM International, pp 279-288.
10. Knott, J.F. *Fundamentals of Fracture Mechanics*, Butterworth, London, 1973, pp 220-221.
11. Petch, N.J. *Acta Metallurgica*, Vol. 34, No 7, 1986, pp.1387-1393.

Table I. Test design matrix and measured properties.

	2% O ₂	5% O ₂	10% O ₂	
Mean inclusion dia. (microns)	0.44	0.52	0.86	As- Welded
Volume fraction (vol. %)	0.175	0.219	0.41	
Avg. Austenite grain width (microns)	333	328	370	
Hardness (DPH)	234-290	225-269	212-258	
Yield Strength (MPa)	696	620	524	
Mean inclusion dia. (microns)	0.44	0.52	0.86	1 Thermal Cycle
Volume fraction (vol. %)	0.175	0.219	0.41	
Avg. Austenite grain width (microns)	30	33	29	
Hardness (DPH)	279	271	244	
Yield Strength (MPa)	*	*	*	
Mean inclusion dia. (microns)	0.44	0.52	0.86	2 Thermal Cycles
Volume fraction (vol. %)	0.175	0.219	0.41	
Avg. Austenite grain width (microns)	20	28	18	
Hardness (DPH)	266	282	245	
Yield Strength (Mpa)	*	*	*	
Mean inclusion dia. (microns)	0.44	0.52	0.86	3 Thermal Cycles
Volume fraction (vol. %)	0.175	0.219	0.41	
Avg. Austenite grain width (microns)	16	25	19	
Hardness (DPH)	279	273	243	
Yield Strength (MPa)	*	*	*	

* = not determined

Table II. Chemical composition, tensile properties, and 50% transformation temperatures (T_{50}).

	C	Mn	Mo	Ni	Cr	Si	Cu	S	P	Al	Ti	N	O	YS	UTS	T_{50}	
	%	%	%	%	%	%	%	%	%	%	%	ppm	ppm	MPa	MPa	°C	
Plate	.034	1.18	.18	3.51	.05	.25	1.25	.002	.008	.035	.01	50	9	---	---		
Weld Metal	2% O ₂	.025	1.23	.51	4.67	.02	.26	0.16	.002	<.004	.003	.009	20	220	696	786	433
	5% O ₂	.024	1.11	.5	4.65	.01	.18	0.19	.002	<.004	.002	.005	40	260	620	724	450
	10% O ₂	.021	1.01	.49	4.59	.02	.19	0.3	.003	<.004	.003	.008	40	470	524	683	473

Table III. Regression statistics for 50% FATT

	<i>Coef.</i>	<i>t Stat</i>	<i>P-value</i>
Intercept	-151.316	-13.1117	3.6E-07
V_f	135.224	5.19552	0.00057
$\ln(\gamma_w)^{-0.5}$	-21.3115	-4.62341	0.00125
R^2	0.85		
V_f = Volume fraction of inclusions			
γ_w = Austenite grain width			

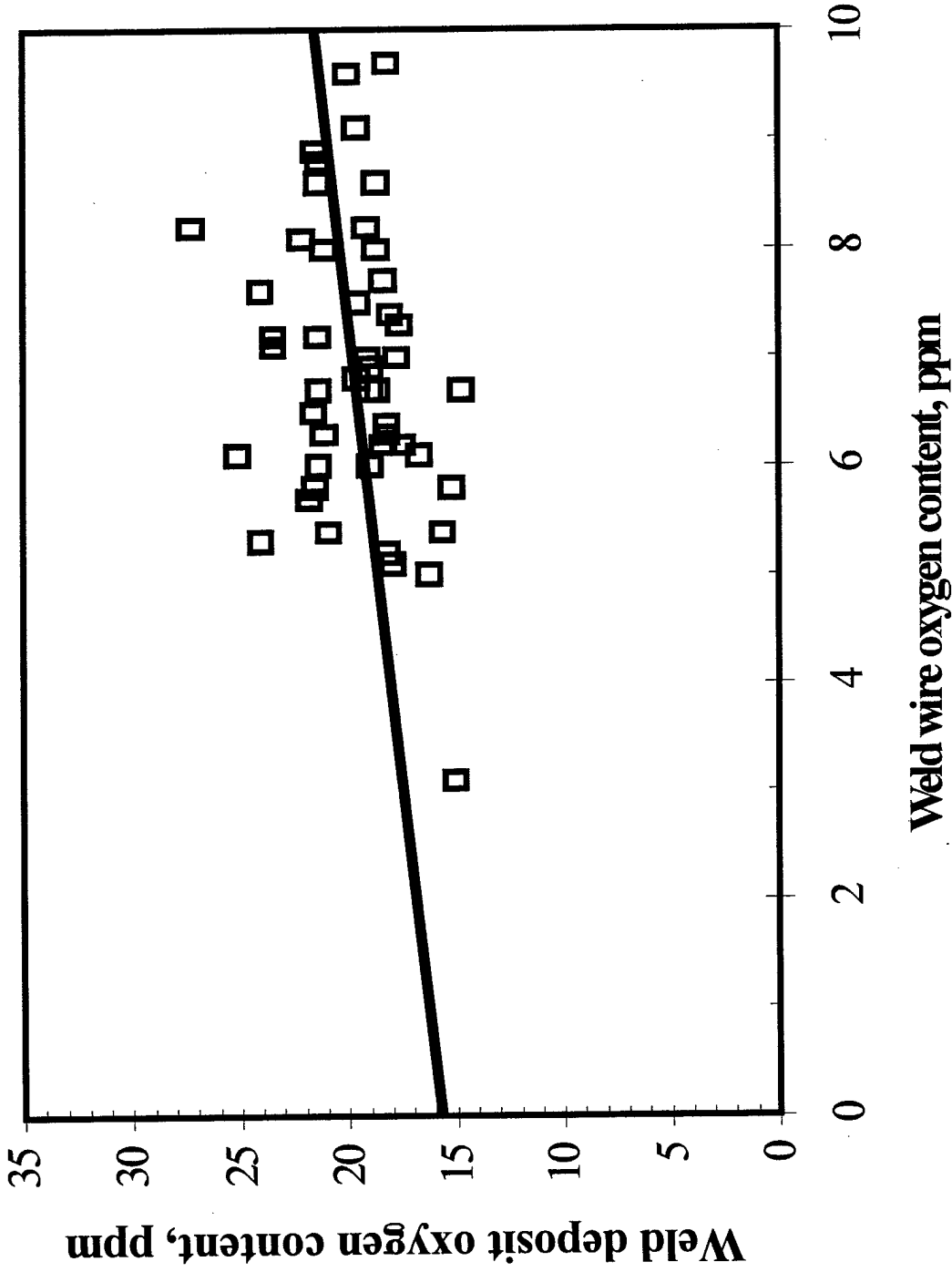


Figure 1. The effect of wire oxygen on weld metal deposit oxygen.

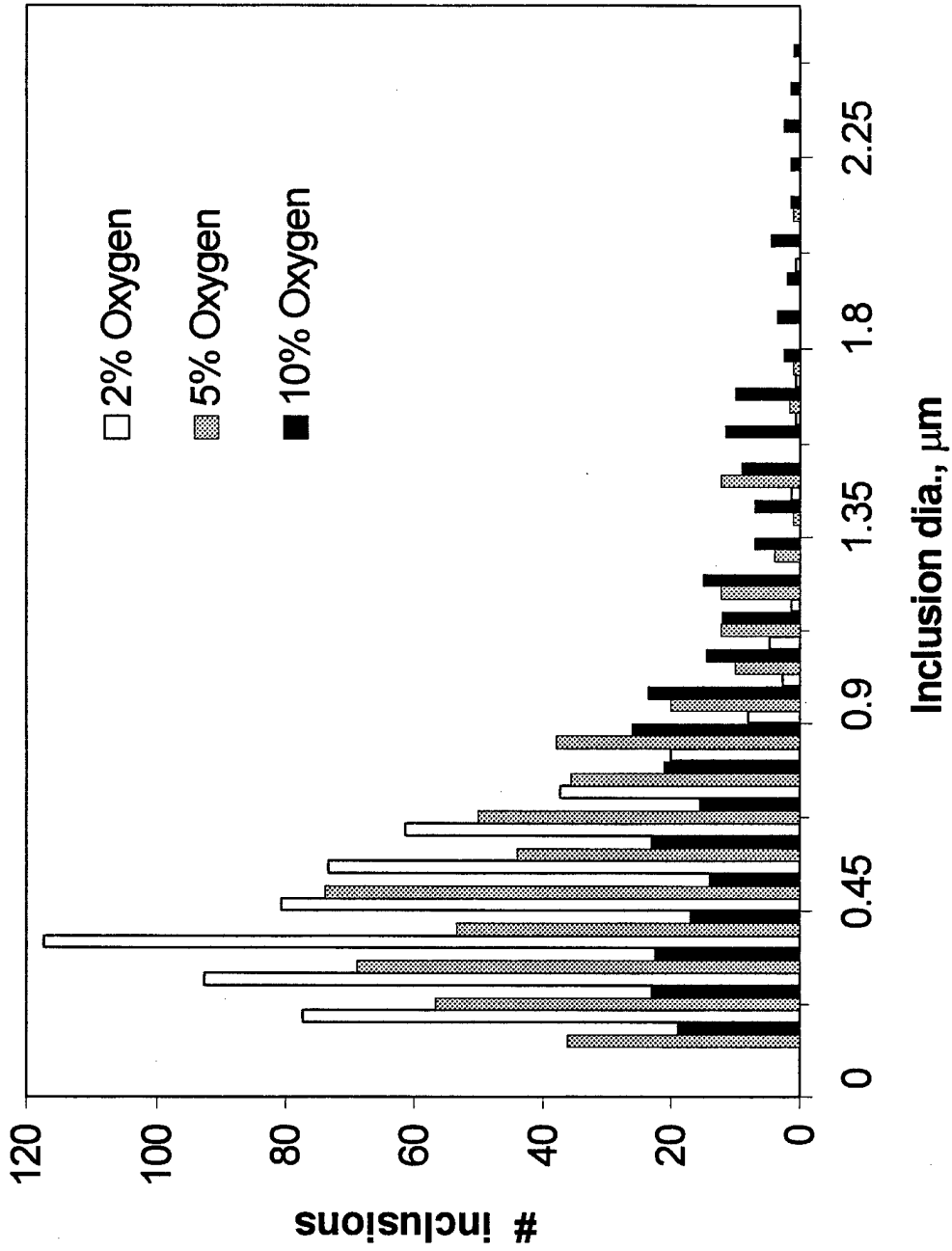


Figure 2. Summary of inclusion data.

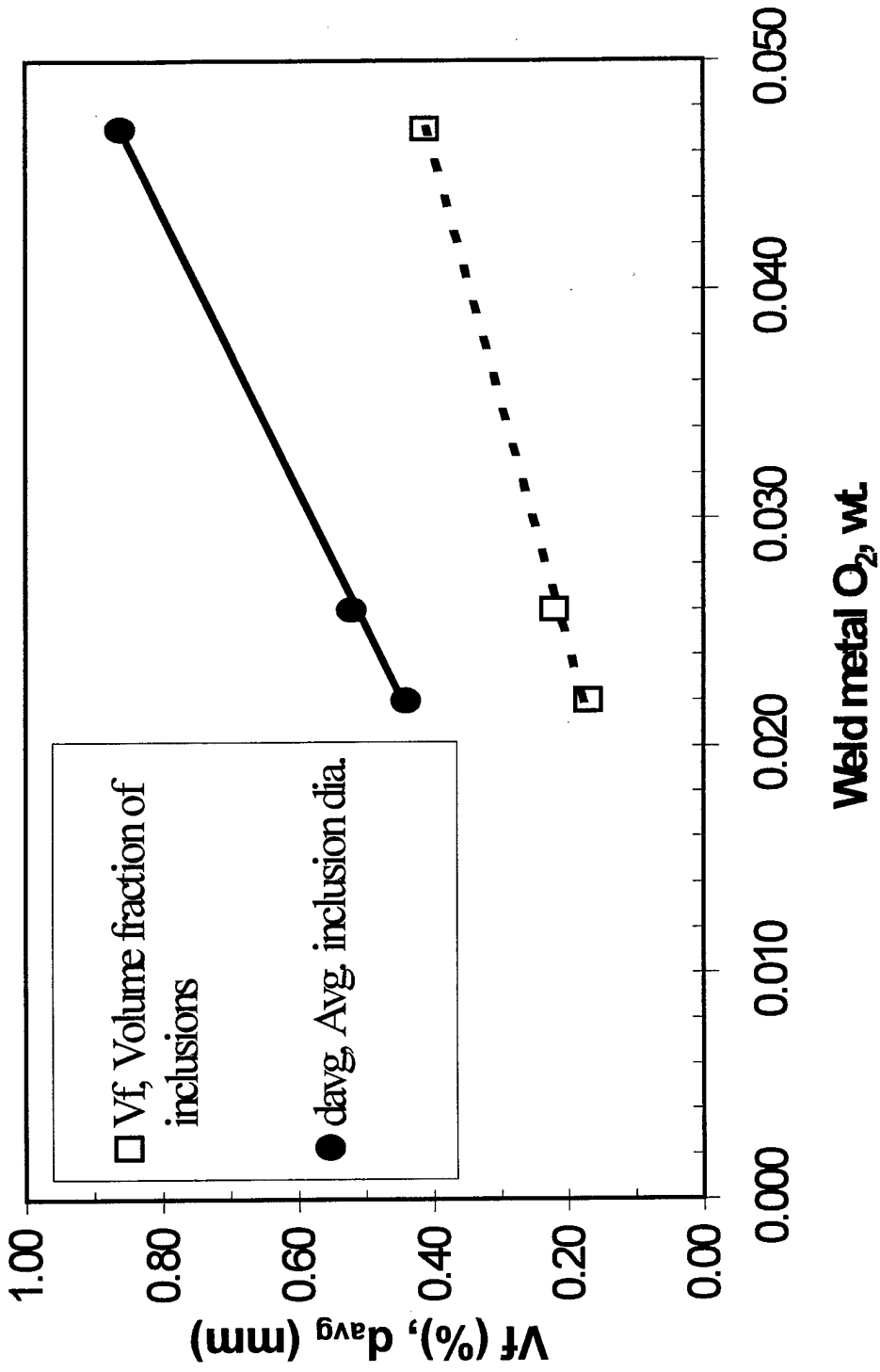


Figure 3. The effect of weld metal oxygen on inclusion characteristics.

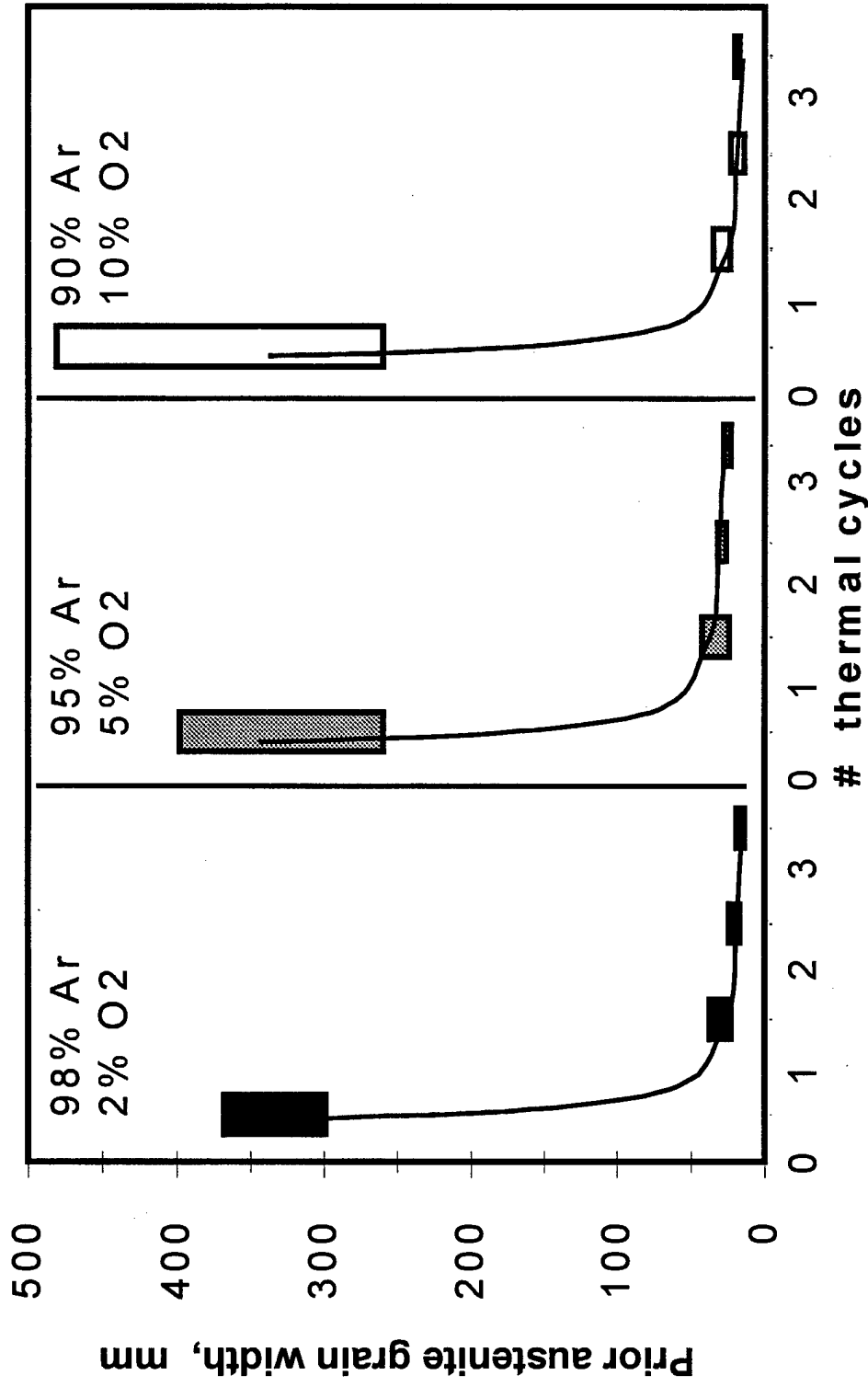


Figure 4. Prior austenite grain width (γ_w) summary.

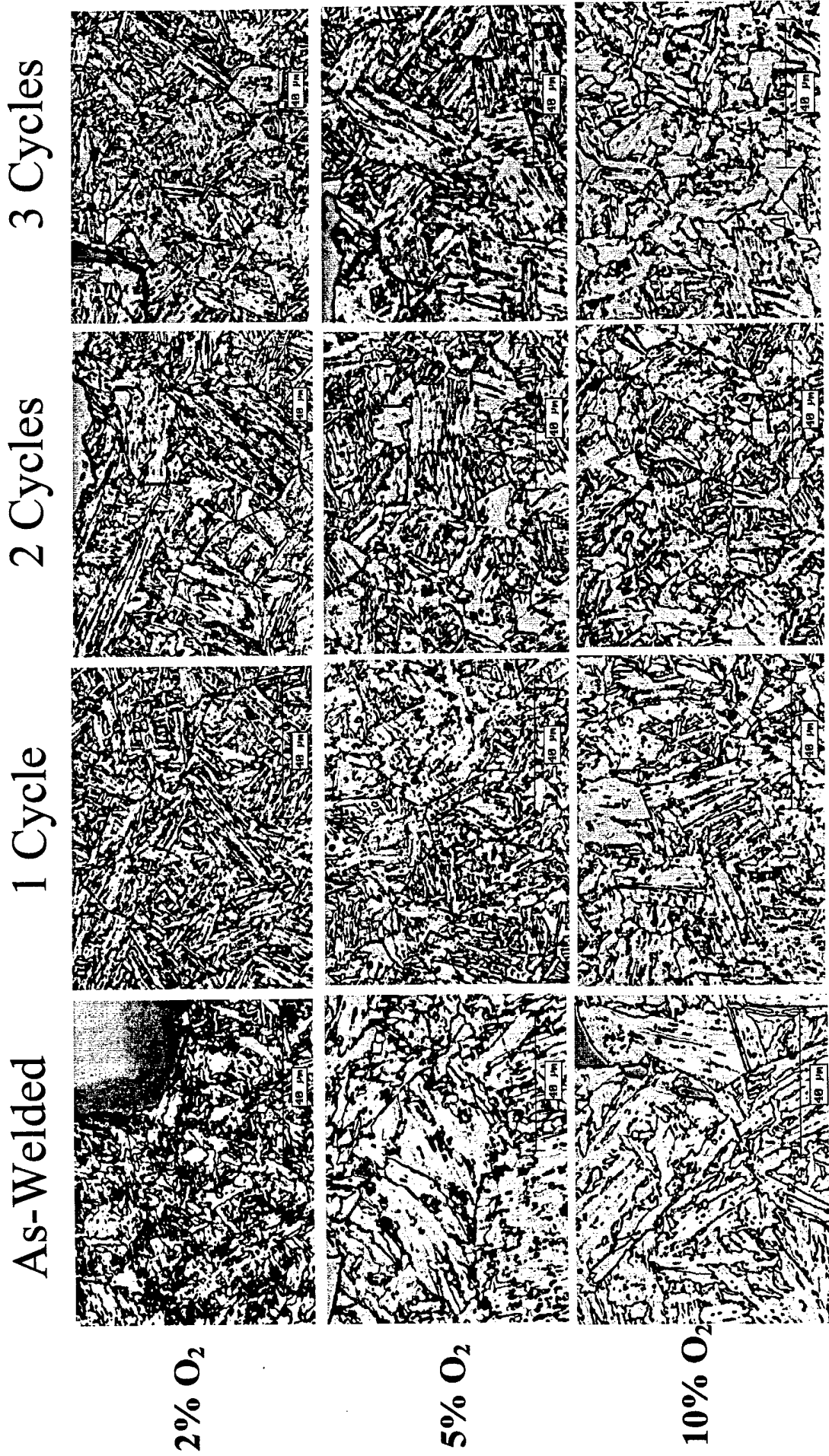


Figure 5. Micrographs of weld metal conditions.

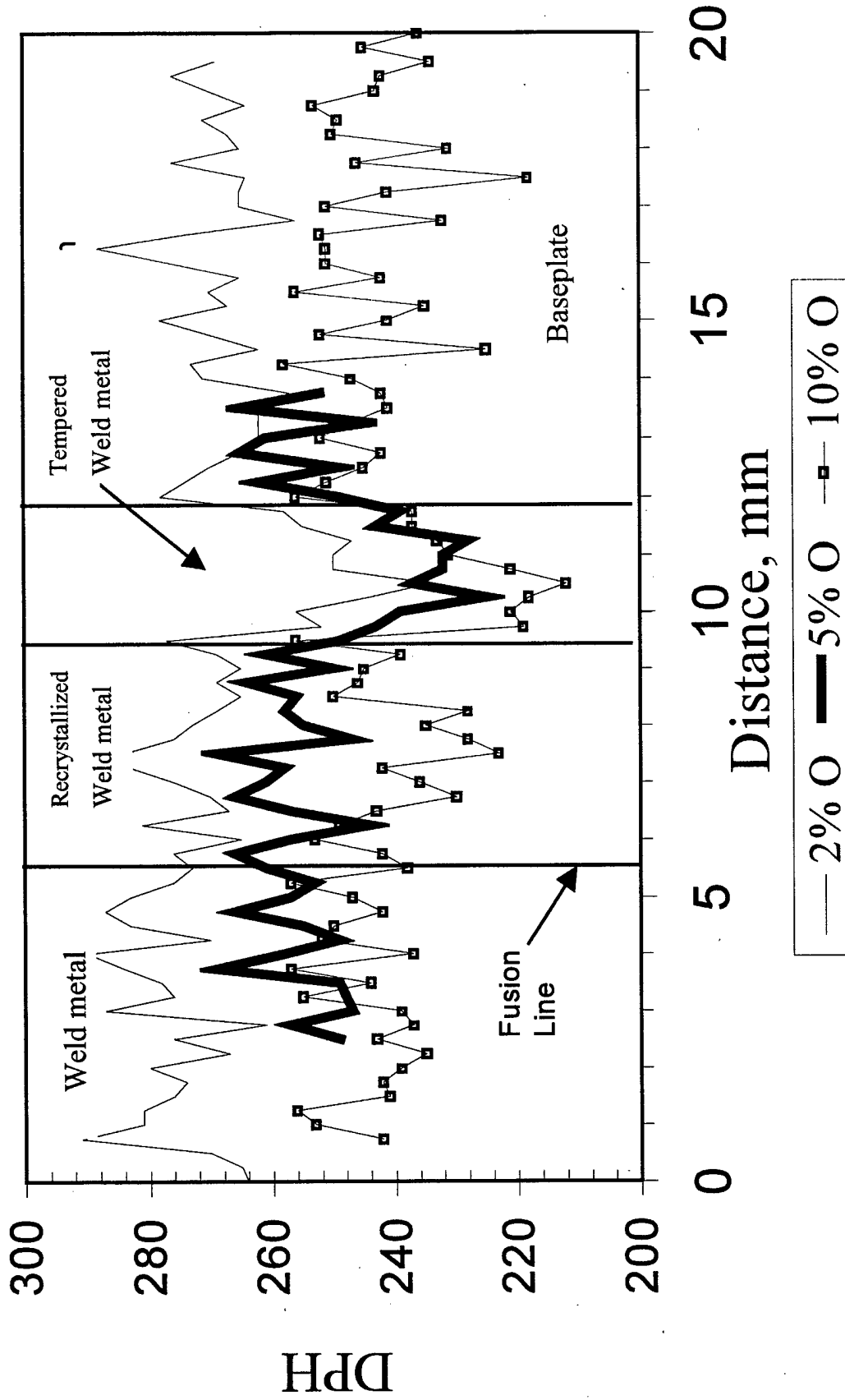


Figure 6. Weld metal hardness profiles with shielding gases containing Ar and 2,5 or 10% O₂.

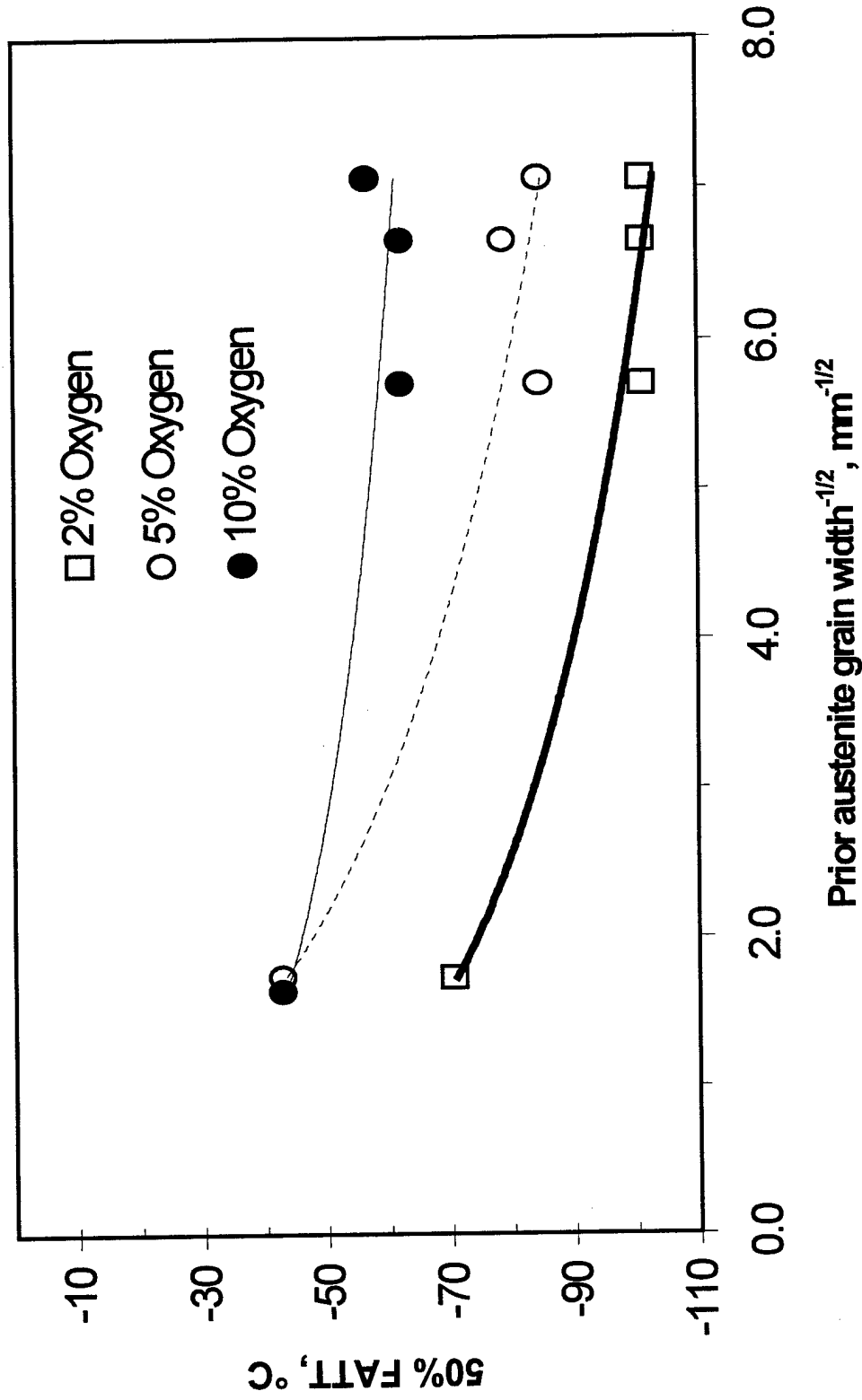


Figure 7. Factors affecting 50% fracture appearance transition temperature (FATT).

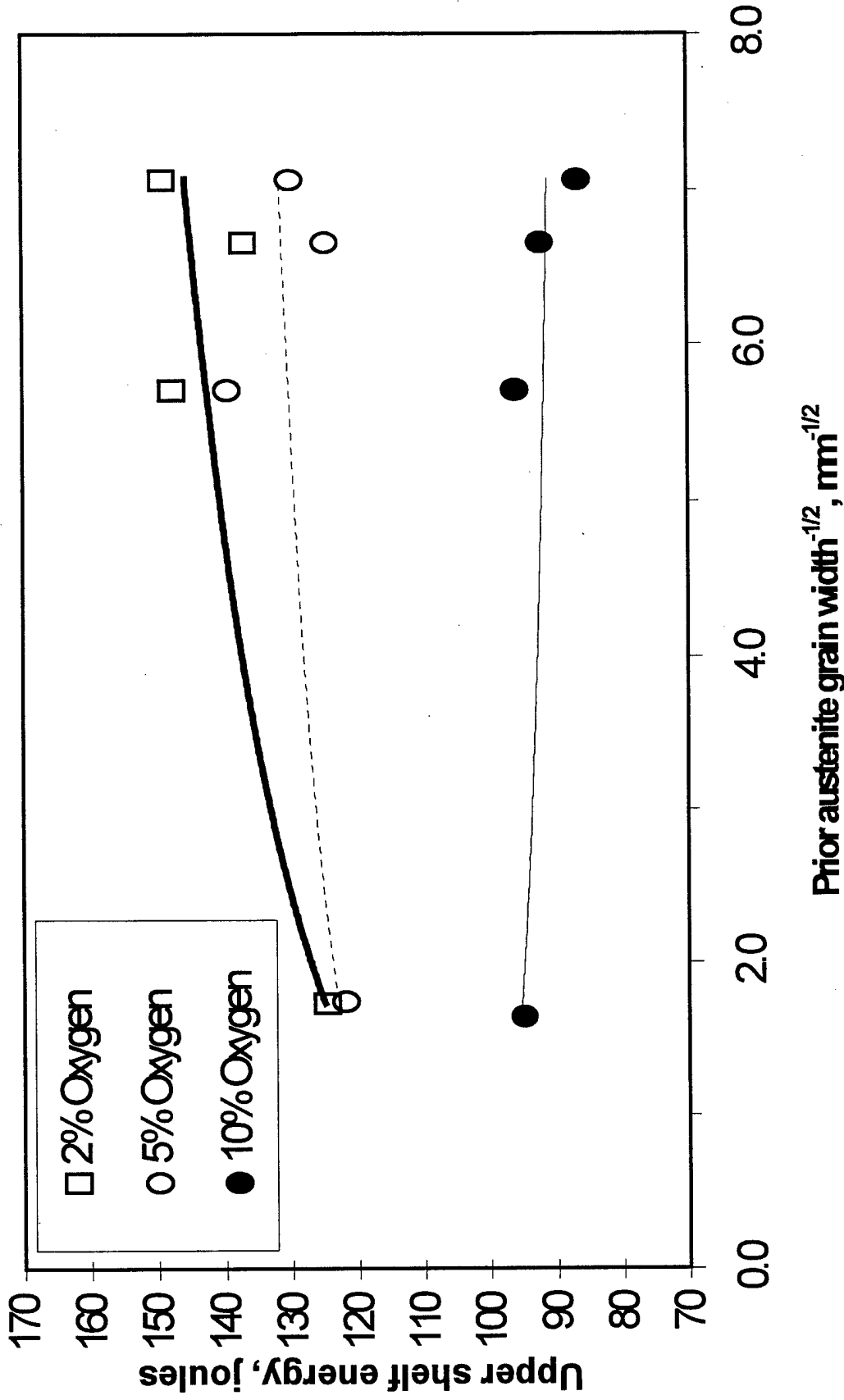
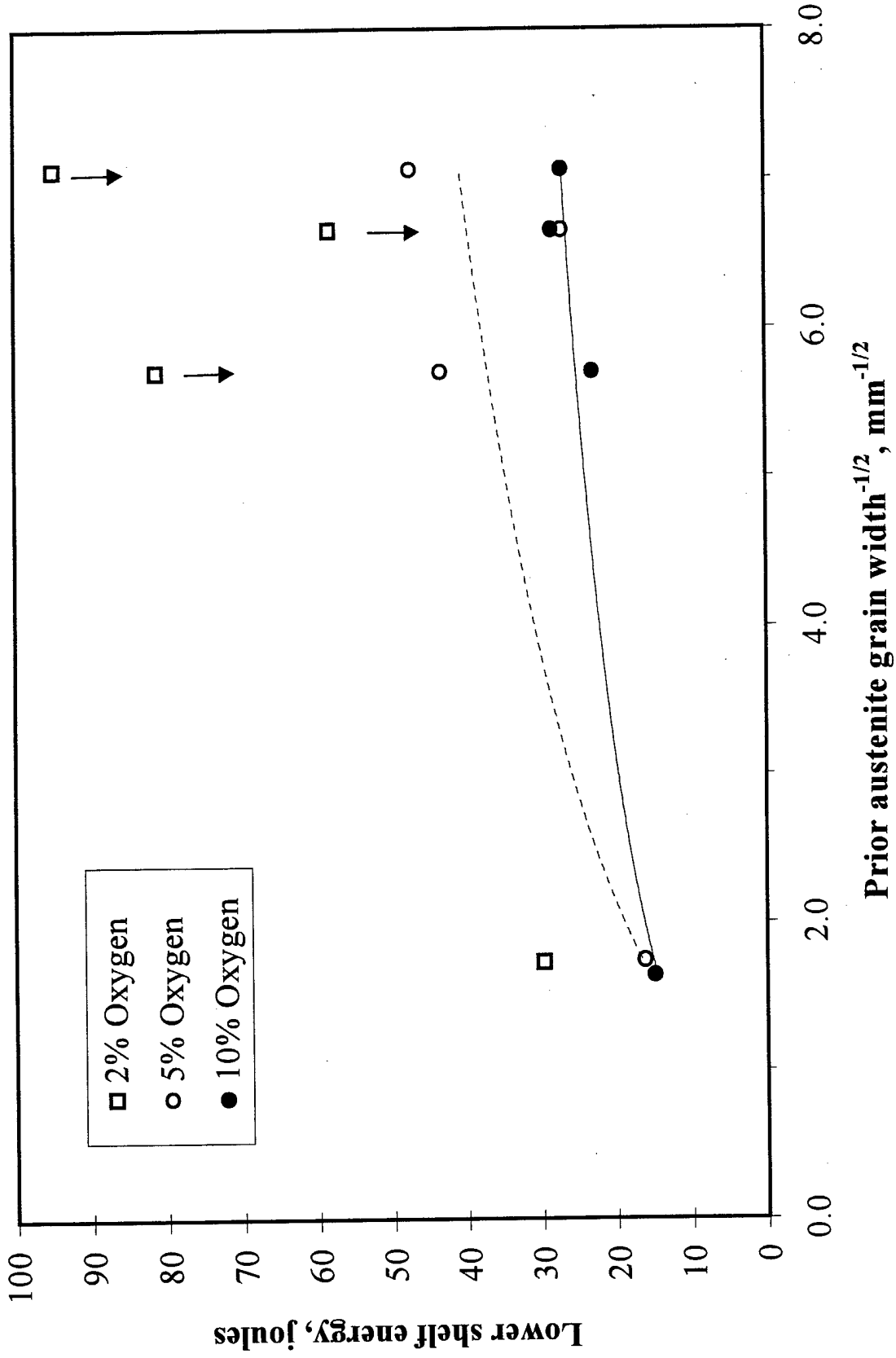


Figure 8. Factors affecting the upper shelf energy.



Prior austenite grain width^{-1/2}, mm^{-1/2}

Figure 9. Factors affecting lower shelf energy.

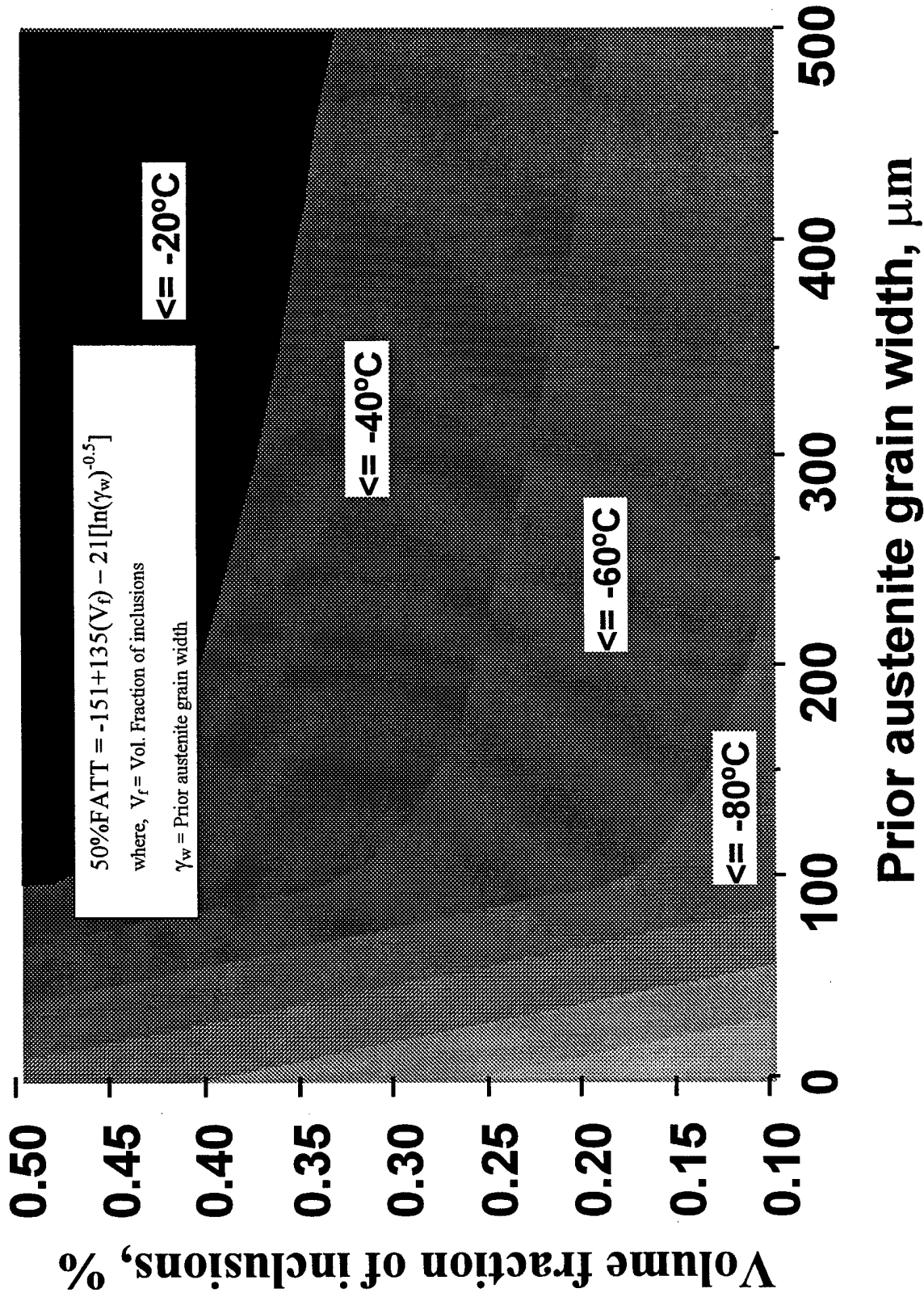
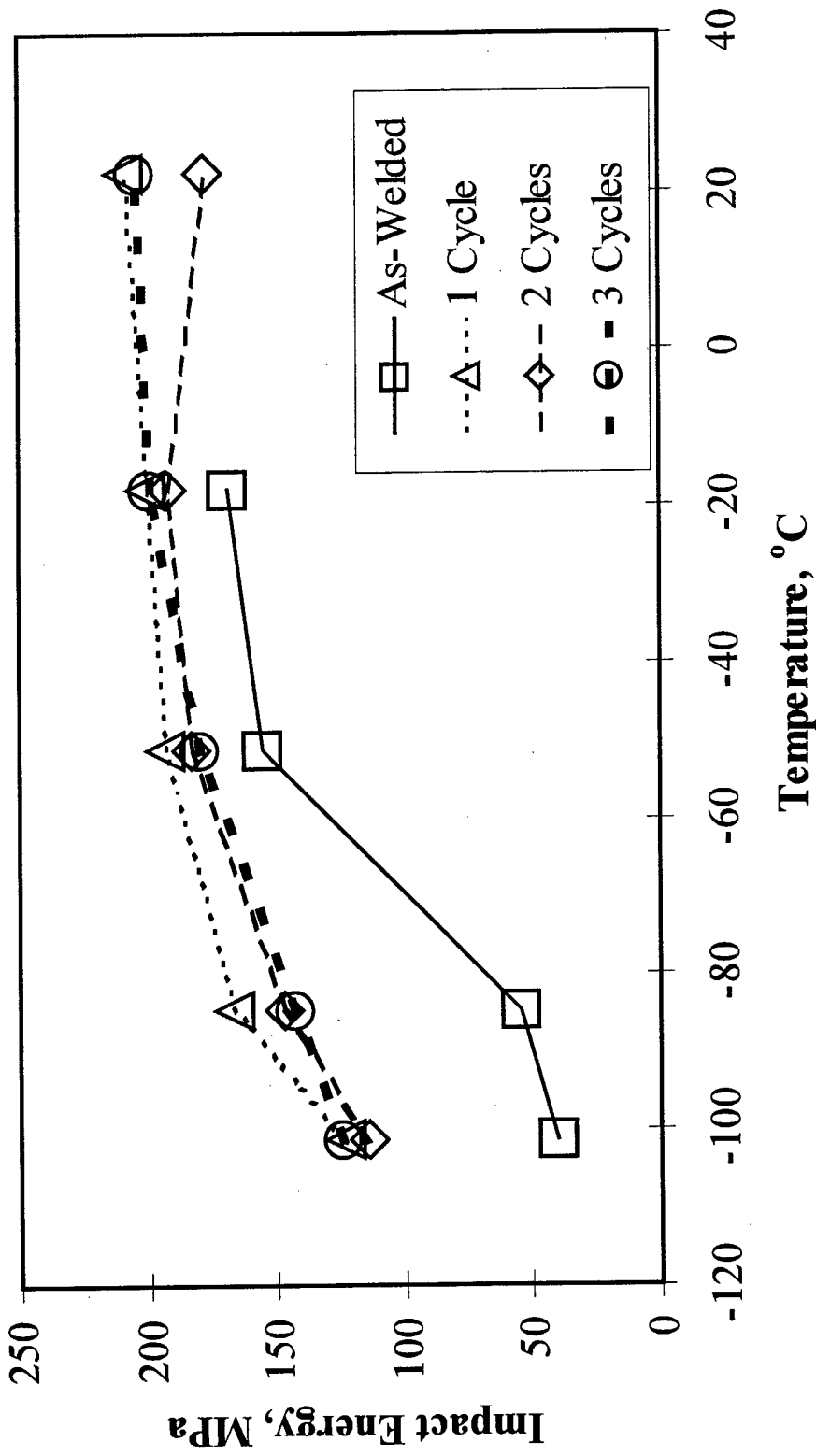


Figure 10. 50% FATT model.

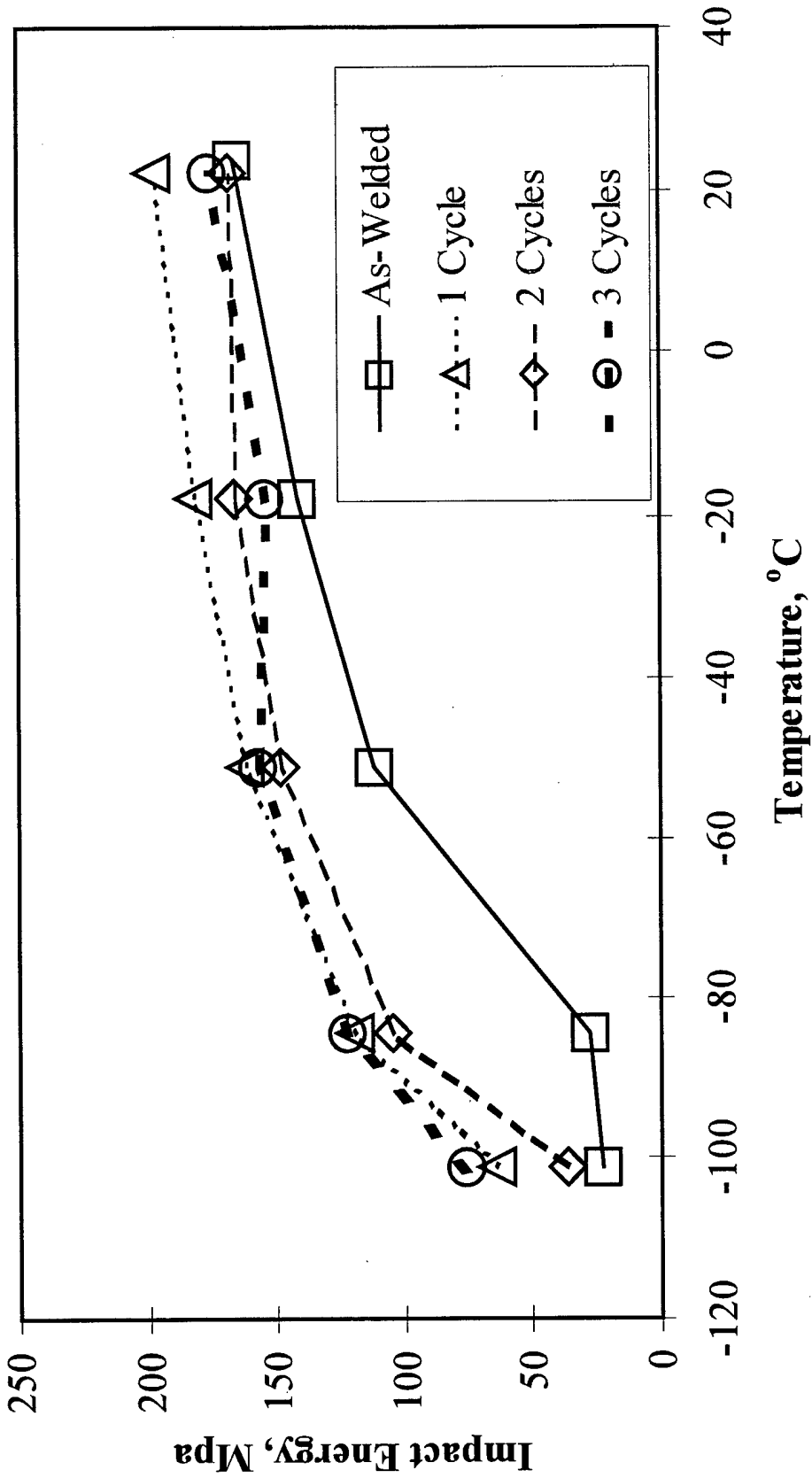
Appendix A - CVN data showing the effects of reheating.

JB-32, 2% Oxygen Effect of Re-Austenitization to 1100°C



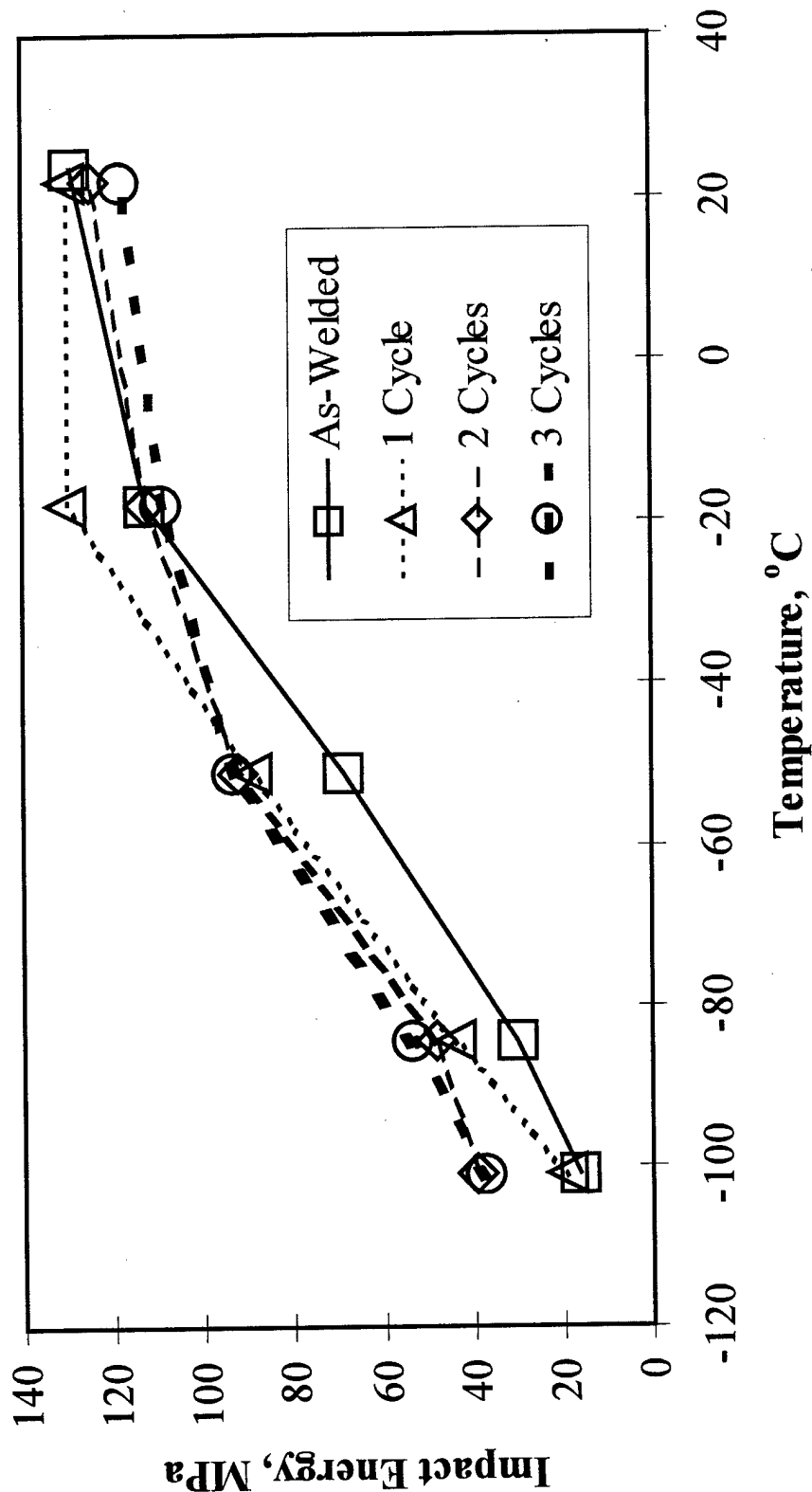
Appendix A - CVN data showing the effects of reheating. (cont'd)

JB-32, 5% Oxygen Effect of Re-Austenitization to 1100°C



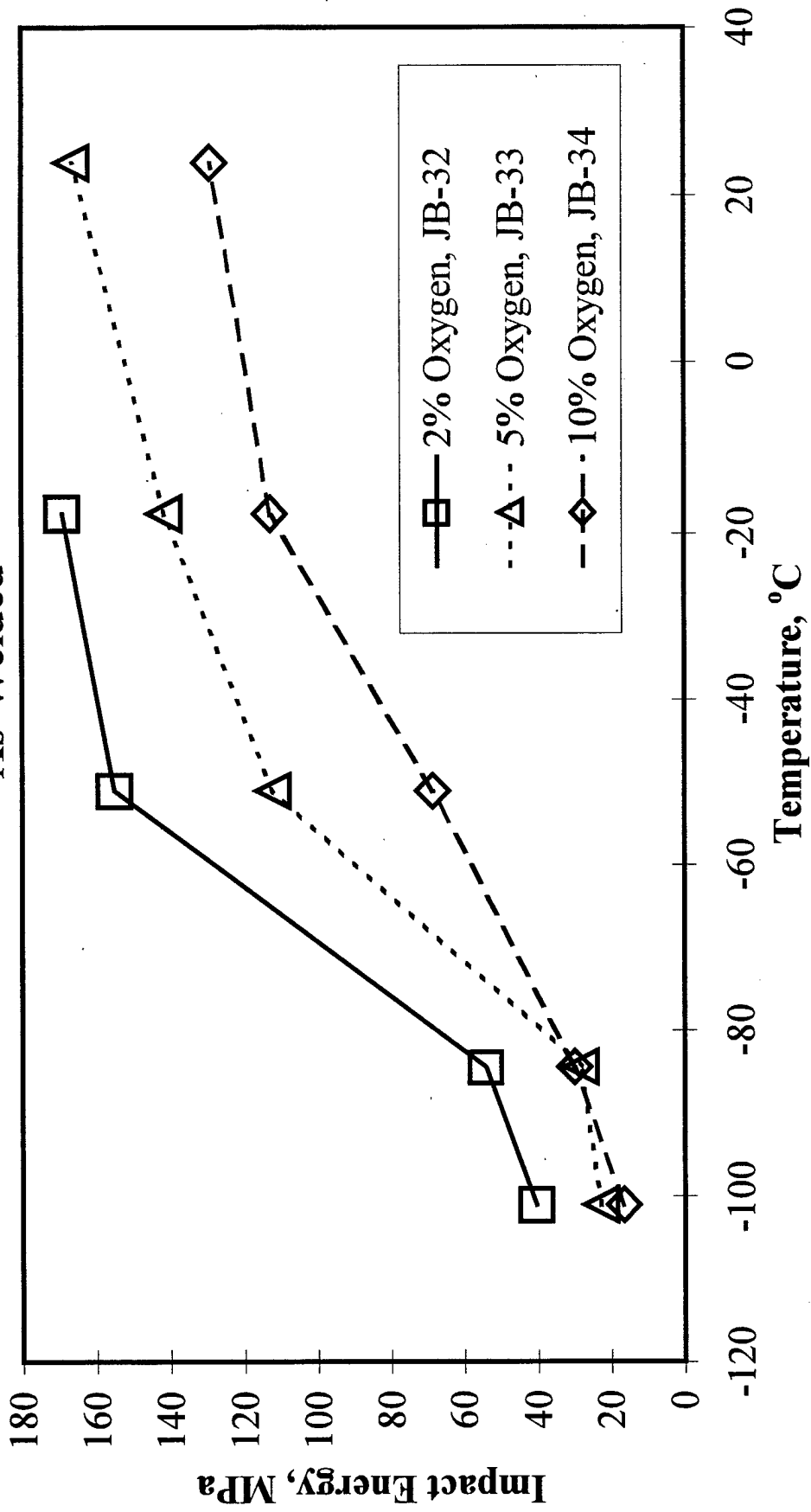
Appendix A - CVN data showing the effects of reheating. (cont'd)

JB-32, 10% Oxygen
Effect of Re-Austenitization to 1100°C



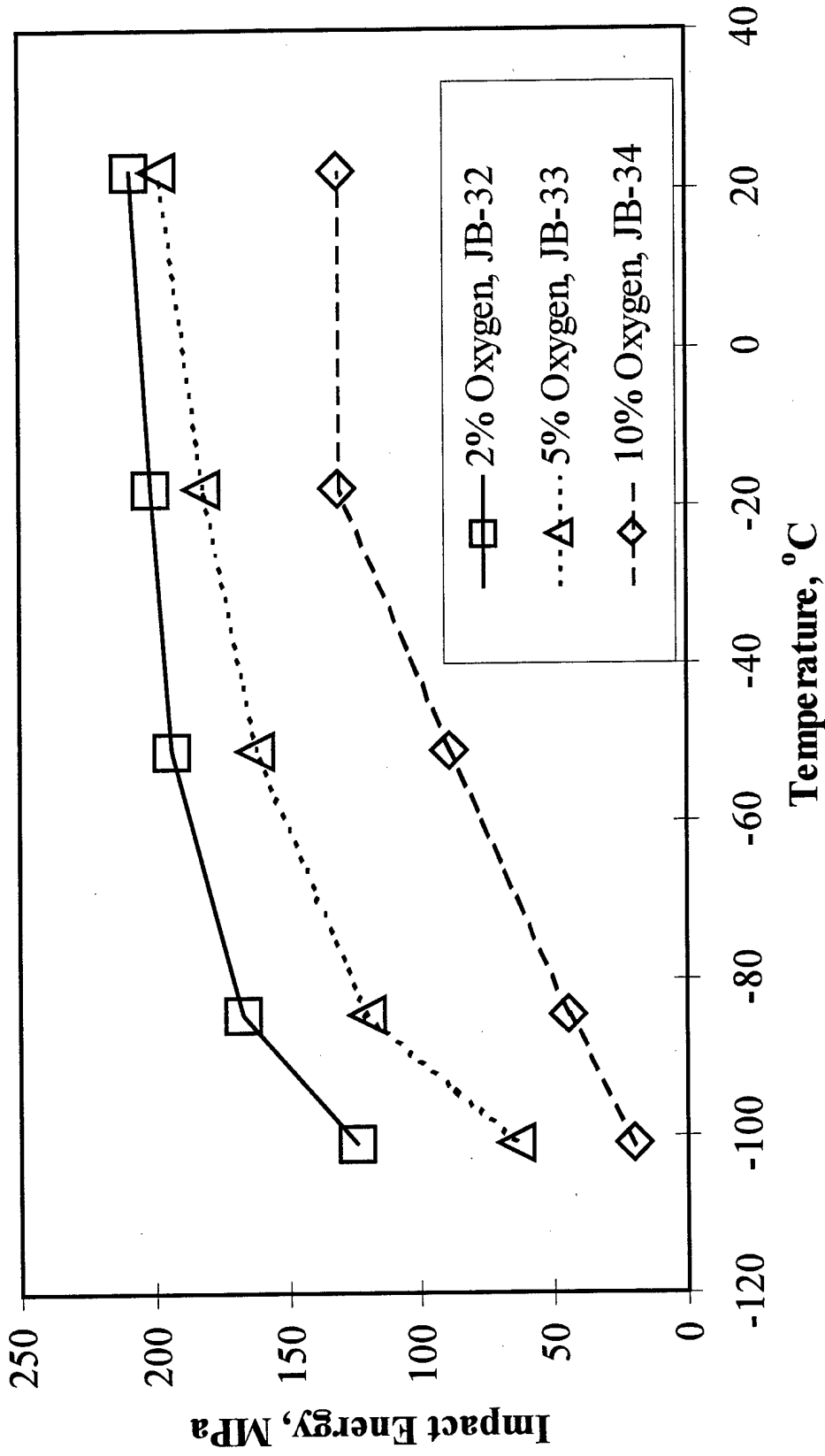
Appendix B - CVN data showing the effects of oxygen.

Effect of Oxygen As-Welded



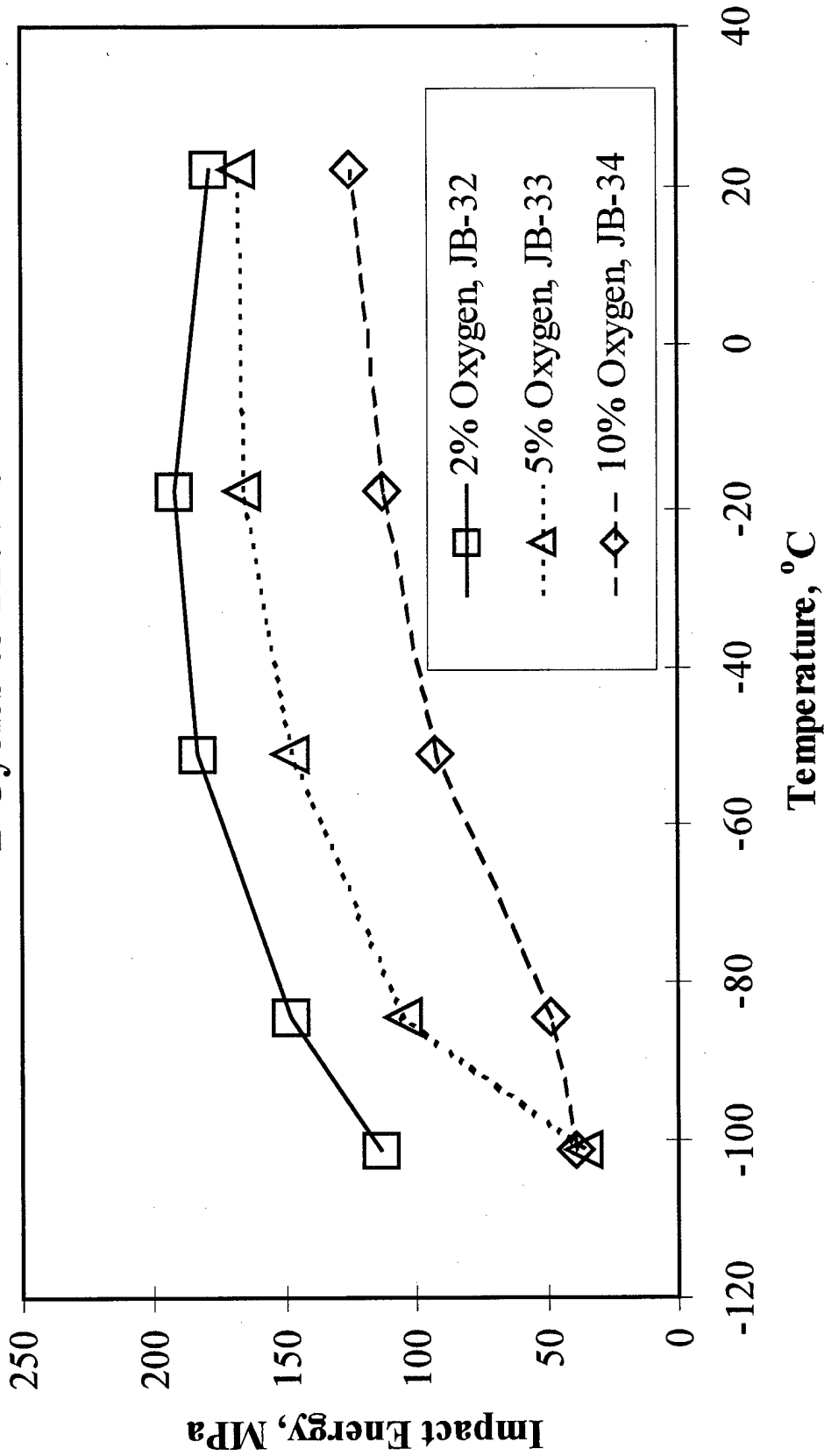
Appendix B - CVN data showing the effects of oxygen (cont'd)

**Effect of Oxygen
1 Cycle to 1100°C**



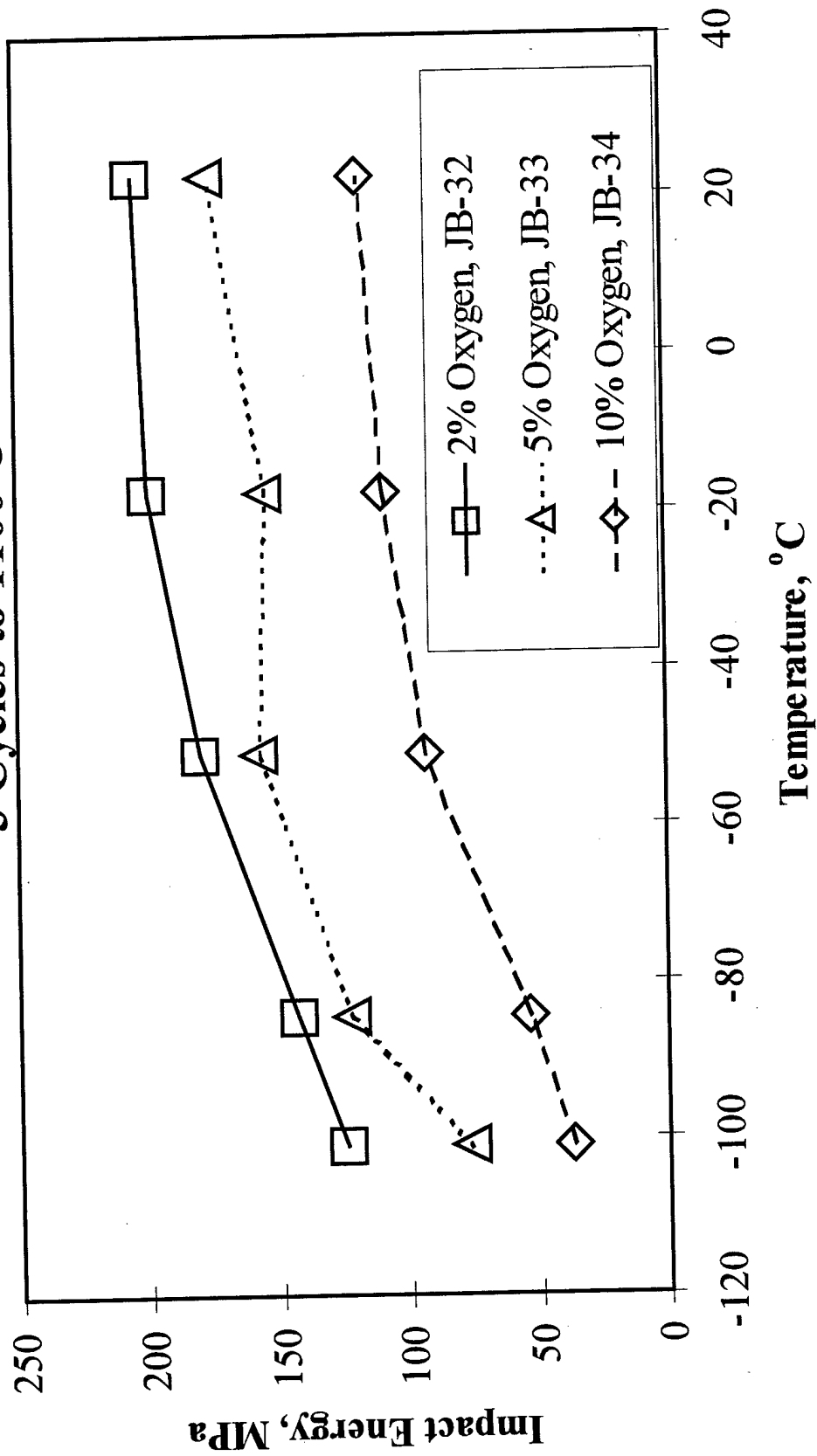
Appendix B - CVN data showing the effects of oxygen (cont'd)

Effect of Oxygen 2 Cycles to 1100°C



Appendix B - CVN data showing the effects of oxygen (cont'd)

Effect of Oxygen 3 Cycles to 1100°C



INITIAL DISTRIBUTION

Copies		DIVISION DISTRIBUTION	
		Copies	Code
2	ONR		
1	Code 332 (Yoder)	1	0115 (Messick)
		1	60
		1	601
6	NAVSEA	1	603
4	SEA 03M2	1	61
2	PMS450T4	1	61s
		1	611
1	NRL	1	612
1	Code 6320	1	613
	Code 6324	1	614
2	DTIC	1	614 (Czyryca)
		1	62
2	National Ctr for Excellence in Metalworking Technology	1	63
		1	64
		1	65
1	Navy Joining Center	1	66
		1	67
2	General Dynamics, Elec Boat Div.	1	68
1	Code D341		
1	Code D470		
			BRANCH DISTRIBUTION
		1	615
2	Newport News Shipbuilding	10	615 (Blackburn)
1	Code 037	1	615 (DeLoach)
1	Code E12	1	615 (Franke)
		1	615 (Wong)
3	ESAB Welding and Cutting Products		
3	Welding Consumables		
1	Hobart Brothers Company		
1	Filler Metal Engineering Dept		
2	Lincoln Electric Company		
2	Consumable Research and Development		
2	Colorado School of Mines		
2	Center for Welding and Joining		
1	Oregon Graduate Institute		
1	Dept of Matls Sci and Engin		